Cluster kinetics and dynamics during spinodal decomposition

Jiao Yang, Benjamin J. McCoy, and Giridhar Madras

Citation: J. Chem. Phys. **124**, 024713 (2006); doi: 10.1063/1.2151900
View online: http://dx.doi.org/10.1063/1.2151900
View Table of Contents: http://jcp.aip.org/resource/1/JCPSA6/v124/i2
Published by the AIP Publishing LLC.

Cluster kinetics and dynamics during spinodal decomposition

Jiao Yang
Department of Chemical Engineering, Louisiana State University, Baton Rouge, Louisiana 70803

Benjamin J. McCoy
Department of Chemical Engineering and Materials Science, University of California, Davis, California 95616

Giridhar Madras[a)]
Department of Chemical Engineering, Indian Institute of Science, Bangalore 560 012, India

(Received 7 October 2005; accepted 22 November 2005; published online 10 January 2006)

Spinodal decomposition (barrierless phase transition) is a spontaneous phase separation caused by conditions that force the system to become thermodynamically unstable. We consider spinodal decomposition to occur under conditions of large supersaturation S and/or small ratio of interfacial to thermal energies ω, such that the computed number of monomers in a critical nucleus $\xi^* = (\omega/\ln S)^3$ is less than unity. The small critical nucleus size is consistent with a negligible energy barrier for initiating condensation. Thus, in contrast to conventional opinion, it is suggested that the spinodal decomposition is related to the homogeneous nucleation of metastable fluids. Population balance equations show how clusters aggregate and rapidly lead to phase separation. Different mass dependences of aggregation rate coefficients are proposed to investigate the fundamental features of spinodal decomposition. When the mass dependency is an integer, the equations are solved by the moment technique to obtain analytical solutions. When the mass dependency is a noninteger, the general cases are solved numerically. All solutions predict the two time regimes observed experimentally: the average length scale of condensed-phase domains increases as a power law with an exponent of 1/3 at early times, followed by a linear increase at longer times. © *2006 American Institute of Physics*. [DOI: 10.1063/1.2151900]

I. INTRODUCTION

Spinodal decomposition is a spontaneous, barrierless phase separation caused by conditions that force the system to become thermodynamically unstable. The process can be understood by visualizing a phase diagram with a coexistence (or binodal) curve (the solid curve in Fig. 1) representing separated phases in equilibrium and ending at a critical point. The binodal encloses a spinodal curve (the dashed curve in Fig. 1), setting the limits of metastability and hence of nucleation. The classical spinodal is the curve on the phase diagram where the critical cluster vanishes.[1] For metastable systems in the region between the binodal and spinodal curves, homogeneous nucleation generates stable clusters that grow by rate-limited processes. When a homogeneous fluid is brought rapidly into the unstable spinodal region, by changing either its temperature or composition, a spontaneous phase separation occurs.[2–5] This condensation has been experimentally studied for the vapor phase,[6] binary alloys,[7] and polymer mixtures.[8] In polymer solutions during phase separation, the polymer-rich phase becomes more viscoelastic with time, causing spinodal decomposition to produce fascinating network structures and patterns.[9] Understanding the phenomenon of spinodal decomposition and its underlying mechanism is pertinent because of its intrinsic importance not only in scientific investigation but also in industrial materials manufacture.

The basic processes in condensation phase transition are nucleation, dispersed cluster growth by reversible monomer deposition, cluster aggregation (coalescence), and Ostwald ripening (coarsening). The critical nucleus size plays a crucial role in these processes, providing the criterion for nucleus formation (homogeneous nucleation) and for nucleus dissolution (denucleation). The premise of this paper is that when the nucleation barrier is vanishingly small, unhindered cluster coalescence dominates the phase transition. According to these notions, the kinetics and dynamics of clusters necessarily underlie condensation phase transitions.

The classical models of phase transitions are developed by Becker and Doring[10] (BD), Lifshitz and Slyozhov[11] (LS), and Wagner[12] (W). The BD model for transitions from the metastable state was based on the formation of clusters by the addition or subtraction of monomers (with no coalescence among larger clusters). The BD equations were generalized[13] to allow the monomer concentrations to vary, with the key restrictive assumption that only monomers can interact with clusters. The LSW theory is concerned with the ripening (coarsening) of the cluster size distribution due to the transfer of mass from smaller less stable clusters to larger more stable clusters, with attendant dissolution of unstable (subcritical) clusters. Marqusee and Ross[14] showed that the LSW solution can be represented as leading terms in an ex-

[a)]Author to whom correspondence should be addressed. Fax: 91-080-2360-0683. Electronic mail: giridhar@chemeng.iisc.ernet.in

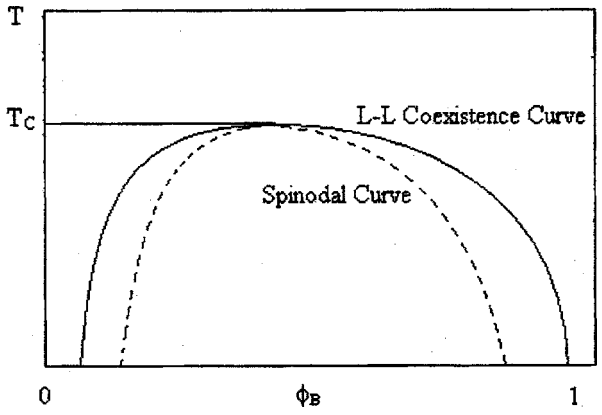

FIG. 1. Schematic phase diagram of a binary mixture where T_c is critical temperature and ϕ_B represents the polymer volume fraction.

pansion of the long-time solution. Further studies of these two classical models of phase transitions, the BD and LSW equations, discussed the connections between them[15] and the different time regimes observed.[16]

For coalescence and breakage, the general model proposed by von Smoluchowski[17] allows clusters of all sizes to aggregate and a cluster to split into unequal fragments. Monette and Klein[18] realized that coalescence of clusters is crucial to the occurrence of spinodal decomposition, the premise that we expand in this work. Unlike condensation from a metastable state, the proposal is that spinodal decomposition occurs when the nucleation energy barrier is negligible, allowing clusters to form and coalesce rapidly. A Smoluchowski-type population balance equation, previously applied to Ostwald ripening[19] and shown to converge[20] to the LSW solutions asymptotically, is applied to model spinodal decomposition.

The Cahn-Hilliard[21,22] theory of spinodal decomposition relies on defining a spinodal curve in terms of the free-energy density $f(c)$ by $[(\partial^2 f/\partial c^2)_T=0]_{c=cs}$. Through its basis in equilibrium thermodynamics, this definition requires a state equation that provides $f(c)$ and is predicated on the existence of equilibrium, at least locally. Concentration fluctuations[23] are supposed to be governed by the collective diffusion coefficient $D=\zeta(\partial^2 f/\partial c^2)_T$, where ζ is a mobility coefficient. In the unstable region, where $(\partial^2 f/\partial c^2)_T<0$, D would be negative and spinodal decomposition is postulated to involve the amplification of a small-amplitude, long-wavelength density or concentration fluctuations caused by thermal fluctuations. The Cahn-Hilliard theory thus enlists a model that is unrelated to and does not transition smoothly from homogeneous nucleation theory, which is fundamental to understanding phase transitions from the metastable state.

Based on a generalization of the liquid-state theory of uniform fluids and on the Fisk-Widom generalization of the thermodynamic theory of van der Waals and Cahn-Hilliard, a theory for the description of the thermodynamics and structure of nonuniform fluids was proposed to analyze the thermodynamic stability of a single-phase fluid in the spinodal region.[24] Molecular dynamics was employed to investigate the time evolution of phase separation by spinodal decomposition in a simulated Lennard-Jones fluid.[25] More recently, Moore *et al.*[26] reported that a two-dimensional Cahn-Hilliard equation was able to model spinodal decomposition of a supersaturated Al–Ag alloy. Through mean-field theories and Monte Carlo simulations of simple lattice models, Frenkel theoretically investigated the interplay of polymer crystallization and liquid-liquid demixing.[27] This interplay results in a shift of the crystallization and liquid-liquid demixing curves in the phase diagram. A kinetic model was proposed, by incorporating the nearest-neighbor pair approximation, to investigate the kinetics of spinodal decomposition for a binary alloy system.[28] The morphology of polymer crystals was dominated by the interplay of polymer crystallization and liquid-liquid demixing. Employing the simple lattice model, Frenkel[29] concluded that the kinetic interplay of spinodal decomposition and polymer crystallization controls the final crystallite morphology. Many small crystallites are produced if crystallization is induced by the prior liquid-liquid phase separation during spinodal decomposition.

The kinetics of spinodal decomposition was experimentally studied by quenching the homogeneous liquid mixture to the unstable region inside the miscibility gap. Jones *et al.*[30] experimentally investigated the segregation of a mixture of poly(ethylenepropylene) (PEP) and perdeuterated PEP (dPEP), which was preferentially wetted by dPEP. Although these experiments showed the formation of the condensed phase, quantitative results for the time dependence of the domain size were not presented. By improving the experimental techniques, Krausch *et al.*[31] investigated a similar system and observed that the growth of the condensed-phase-domain size follows the power-law dependence $R(t) \sim t^{1/3}$. Bulk phase separation, where fluid is driven by advective transport along the domain boundaries, yields faster growth of the phase domain size. Other experimental studies[32] presented a fast mode of condensed-phase growth in polymer and fluid mixtures.

In simple fluid systems, two time regimes are observed.[33] At relatively early times, the time variation of the condensed-phase-domain size is a power law with an exponent of 0.3–0.4; at longer times the variation becomes linear, i.e., the exponent becomes unity. The early time regime is supposed to be diffusion dominated because diffusion governs material transport in homogeneous liquids. At longer times, the newly formed condensed phase establishes density differences between the two phases and causes convection to be the driving force.[34] By incorporating hydrodynamic effects, the phase separation can be modeled at both the microscopic and coarsed-grain levels.[35–37] Guenoun *et al.*[38] reported that domain growth parallel to the surface was slower than bulk growth and was characterized by a growth exponent of 0.5-0.7. Bray[39] summarized the growth law for the condensed phase in different regimes with growth exponents of 1/2, 1, and 2/3 as diffusive, viscous, and inertial hydrodynamic regimes, respectively. The analytical, numerical, and experimental investigations of spinodal decomposition have been extensively reviewed.[35–37,40]

The objective of this study is to investigate the kinetics of phase separation during spinodal decomposition. A cluster-size-distribution model, previously applied to Ostwald ripening[19] and polymer crystallization, is used to model these phenomena. It is shown that the model, by including

aggregation, successfully simulates spinodal decomposition and exhibits the two time regions observed experimentally for the evolution of the average size of the dense phase domains.

II. DISTRIBUTION KINETICS

Spinodal decomposition can be conceptualized in the context of general phase-transition dynamics and can be considered as a limiting case that occurs when the fluid is unstable. In contrast to conventional theories that are unrelated to and do not transition smoothly from homogeneous nucleation theory, it is suggested that the process smoothly connects with nucleated condensation of metastable fluids. Classical nucleation theory[41,42] accounts for nucleation rate by means of the cluster energy W as a function of cluster radius r expressed in terms of temperature T, interfacial energy σ, monomer molar volume x_m/ρ, and supersaturation S,

$$W(r) = 4\pi r^2\sigma - (4/3)\pi r^3(\rho/x_m)k_BT \ln S. \tag{1}$$

The mass x of a spherical condensate cluster is related to the cluster mass density ρ and the radius r by $x=(4/3)\pi r^3\rho$. The cluster energy reaches a maximum value W^* at the critical cluster radius r^*,

$$r^* = 2\sigma x_m/\rho k_BT \ln S. \tag{2}$$

Thus by Eq. (2), the energy barrier for nucleation is

$$W^* = (16/3)x_m^2\pi\sigma^3/(\rho k_BT \ln S)^2. \tag{3}$$

The critical cluster mass x^* may be scaled in units of monomer mass x_m,

$$\xi^* = x^*/x_m = (\omega/\ln S)^3, \tag{4}$$

where

$$\omega = (4\pi x_m^2/3\rho^2)^{1/3}2\sigma/k_BT \tag{5}$$

is the ratio of monomer interfacial energy to thermal energy k_BT and plays a key role in controlling nucleation, growth, and ripening.[43] The classical expression[42] for the nucleation rate (nuclei/volume$\times$time) is the flux over the maximum energy barrier (at $r=r^*$),

$$I = k_n \exp(-W^*/k_BT), \tag{6}$$

prefactor with the prefactor

$$k_n = (m^{(0)})^2(2\sigma x_m/\pi)^{1/2}/\rho, \tag{7}$$

where $m^{(0)}$ is the monomer concentration. The supersaturation is defined by

$$S = m^{(0)}/m_\infty^{(0)}, \tag{8}$$

where $m_\infty^{(0)}$ is the monomer concentration in equilibrium with its plane ($r\to\infty$) condensed phase. For nucleation of a metastable vapor, the number of monomers in the critical nucleus ξ^* is typically greater than 10, and nucleation precedes cluster growth. According to Eq. (4), however, for sufficiently small ω and large S, the nucleus critical size is smaller than a monomer ($\xi^*<1$) when the solution is brought into the spinodal region by changing its temperature and composition. This unrealistic critical nucleus size indicates that, unlike nucleation of a metastable vapor, spinodal decomposition does not involve a nucleation barrier mechanism because the monomer (molecule in the solution) is larger than the critical nucleus. According to this view, spinodal decomposition is actually condensation by cluster aggregation in the solution.

Experiments show that small microdomains or clusters rapidly appear and grow by diffusion and coalescence until they become large enough to sediment.[44] The hypothesis of the present investigation is prompted by these observations. As the supersaturation increases, or (less likely) the interfacial energy decreases, the critical nucleus size ξ^* decreases. When $\xi^*<\sim 1$, the concept of a smallest stable cluster loses its meaning, and condensation has no nucleation barrier. At such high values of S, the density or concentration of the fluid is large enough that an aggregation process, similar to step polymerization, can occur. Thus, monomers combine to form dimers, dimers combine with monomers or with other dimers, the resulting trimers or tetramers combine with other clusters, and so on. By means of this cascading coalescence, in addition to diffusion-influenced monomer addition to clusters (growth), the fluid rapidly condenses. Going beyond mean-field theories that are based on thermodynamic equations of state, the present model is thus based on heterogeneous cluster kinetics and dynamics. Through its dependence on supersaturation, the hypothesized process allows a smooth transition between the theories of homogeneous nucleation and spinodal decomposition. Homogeneous nucleation with reversible cluster growth has been applied previously to crystal growth in polymer crystallization.[45–47]

Since the critical cluster size is less than one molecule, the condensation, according to the pattern evolution of spinodal decomposition,[34] can be represented as a reversible aggregation-fragmentation process for clusters,

$$C(x) + C(x') \underset{k_b}{\overset{k_a}{\rightleftarrows}} C(x+x'), \tag{9}$$

where $C(x)$ represents a cluster having mass of x, k_a stands for the aggregation rate coefficient, and k_b stands for fragmentation rate coefficient. We assume that monomer-cluster interactions are negligible.

The population balance equations that govern the distribution of the clusters, $c(x,t)$, is based on mass conservation for the processes represented by Eq. (9):

$$\begin{aligned}\partial c(x,t)/\partial t = &-2c(x,t)\int_0^\infty k_a(x,x')c(x',t)dx' \\ &+ \int_0^x k_a(x',x-x')c(x',t)c(x-x',t)dx' \\ &- k_b(x)c(x,t) + 2\int_x^\infty k_b(x')c(x',t)dx'.\end{aligned} \tag{10}$$

Integral forms of the rate expressions in the population balance equation lead themselves to the calculation of moments, defined as integrals over x,

$$c^{(n)}(t) = \int_0^\infty c(x,t)x^n dx. \tag{11}$$

The zeroth moment $c^{(0)}(t)$ is the time-dependent molar concentration of clusters, and the first moment $c^{(1)}(t)$ is mass concentration (mass/volume). The average cluster mass is the ratio

$$c^{\text{avg}} = c^{(1)}/c^{(0)}. \tag{12}$$

In general both rate coefficients k_a and k_b are functions of cluster mass, as well as temperature and other local thermodynamic state conditions. If we consider them as constants, applying the moment operation implied by Eq. (10) yields

$$dc^{(n)}/dt = -2k_a c^{(0)}c^{(n)} + k_a \sum_{j=0}^{n} (n_j)c^{(j)}c^{(n-j)} - k_b c^{(n)} + 2k_b c^{(n)}/(n+1). \tag{13}$$

It follows that the cluster moment equations for $n=0$ and 1 are

$$dc^{(0)}/dt = k_a(k_b/k_a - c^{(0)})c^{(0)} \tag{14}$$

and

$$dc^{(1)}/dt = 0, \tag{15}$$

where Eq. (15) is the mass balance. The initial condition is molar concentration $c_0^{(0)}$(of monomers), which gives the constant mass concentration

$$c_0^{(1)} = x_m c_0^{(0)}. \tag{16}$$

To satisfy microscopic reversibility (detailed balance), the local equilibrium condition for Eq. (14) imposes

$$k_b/k_a = c_{\text{eq}}^{(0)}. \tag{17}$$

According to experimental observations, however, all the clusters finally aggregate into one continuous dense phase (or a relatively few clusters), $c_{\text{eq}}^{(0)} \approx 0$. It can be concluded that the fragmentation rate coefficient is relatively small, $k_a \gg k_b$, and fragmentation can be neglected in Eq. (10). We therefore focus on an irreversible aggregation model.

As mentioned, the aggregation rate coefficient is a function of the masses of combining clusters. Previous studies[48] have considered $k_a(x,x') = \kappa(xx')^a$ or $(x+x')^b$. Here, the rate coefficient is represented as a general power-law form,

$$k_a(x,x') = \kappa(xx')^\mu (x+x')^\nu, \tag{18}$$

where the aggregation rate coefficient prefactor κ and the powers μ and ν are constants. Dimensionless quantities are scaled by the prefactor κ and the molecular weight x_m,

$$\xi = x/x_m, \quad \theta = t\kappa {x_m}^{2\mu+\nu}, \quad C(\xi,\theta) = c(x,t)x_m, \tag{19}$$

where ξ is the number of monomers in the cluster and $C(\xi,\theta)d\xi$ represents the number of dense phase domains including molecules in the range $(\xi, \xi+d\xi)$ at time θ. Based on the dimensionless quantities, the population balance equation [Eq. (10)] neglecting fragmentation can be written as

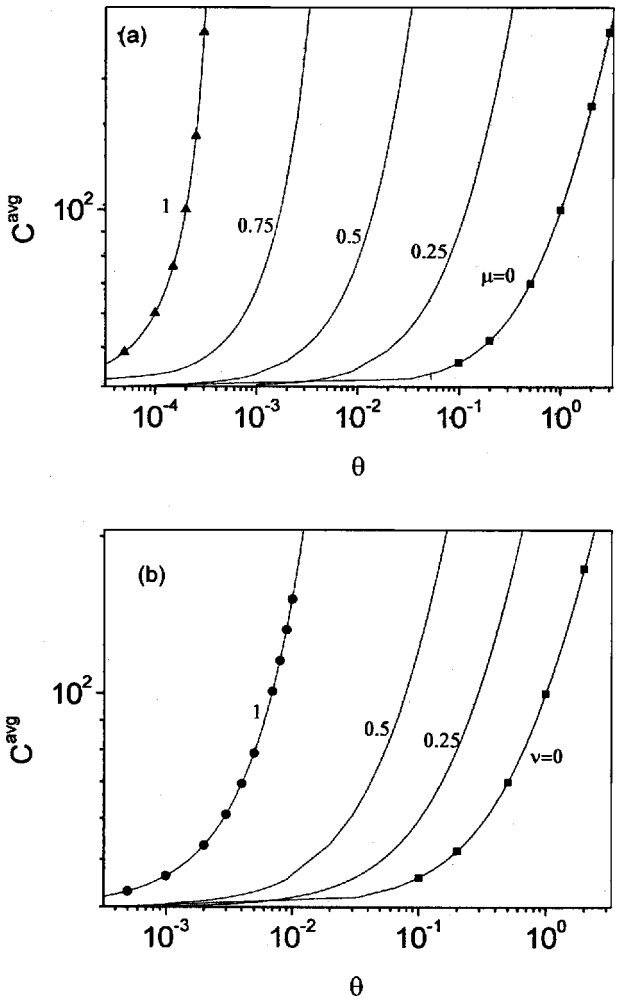

FIG. 2. Effect of (a) μ with $\nu=0$ and (b) ν with $\mu=0$ on the time evolution of C^{avg} with $C_0^{(0)}=1$ and $C_0^{\text{avg}}=50$. The points represent the analytical solutions and the lines represent the numerical solution.

$$\partial C(\xi,\theta)/\partial\theta = -2\xi^\mu C(\xi,\theta)\int_0^\infty \xi'^\mu(\xi+\xi')^\nu C(\xi',\theta)d\xi' + \xi^\nu \int_0^\xi (\xi-\xi')^\mu \xi'^\mu C(\xi',\theta)C(\xi-\xi',\theta)d\xi'. \tag{20}$$

Similarly, the nth moment of dense phase domains can be rewritten into a dimensionless form,

$$C^{(n)}(\theta) = \int_0^\infty C(\xi,\theta)\xi^n d\xi. \tag{21}$$

Applying the moment operation to Eq. (20) for integer values of n and ν yields

$$dC^{(n)}/d\theta = -2\sum_{j=0}^{\nu} \binom{\nu}{j} C^{(n+\mu+j)}C^{(\mu+\nu-j)} + \sum_{j=0}^{n+\nu} \binom{n+\nu}{j} C^{(\mu+j)}C^{(n+\mu+\nu-j)}. \tag{22}$$

For $n=1$, $dC^{(1)}/d\theta=0$ for all values of μ and ν, indicating conservation of mass, $C^{(1)}(\theta)=C_0^{(1)}$. The simplest case,

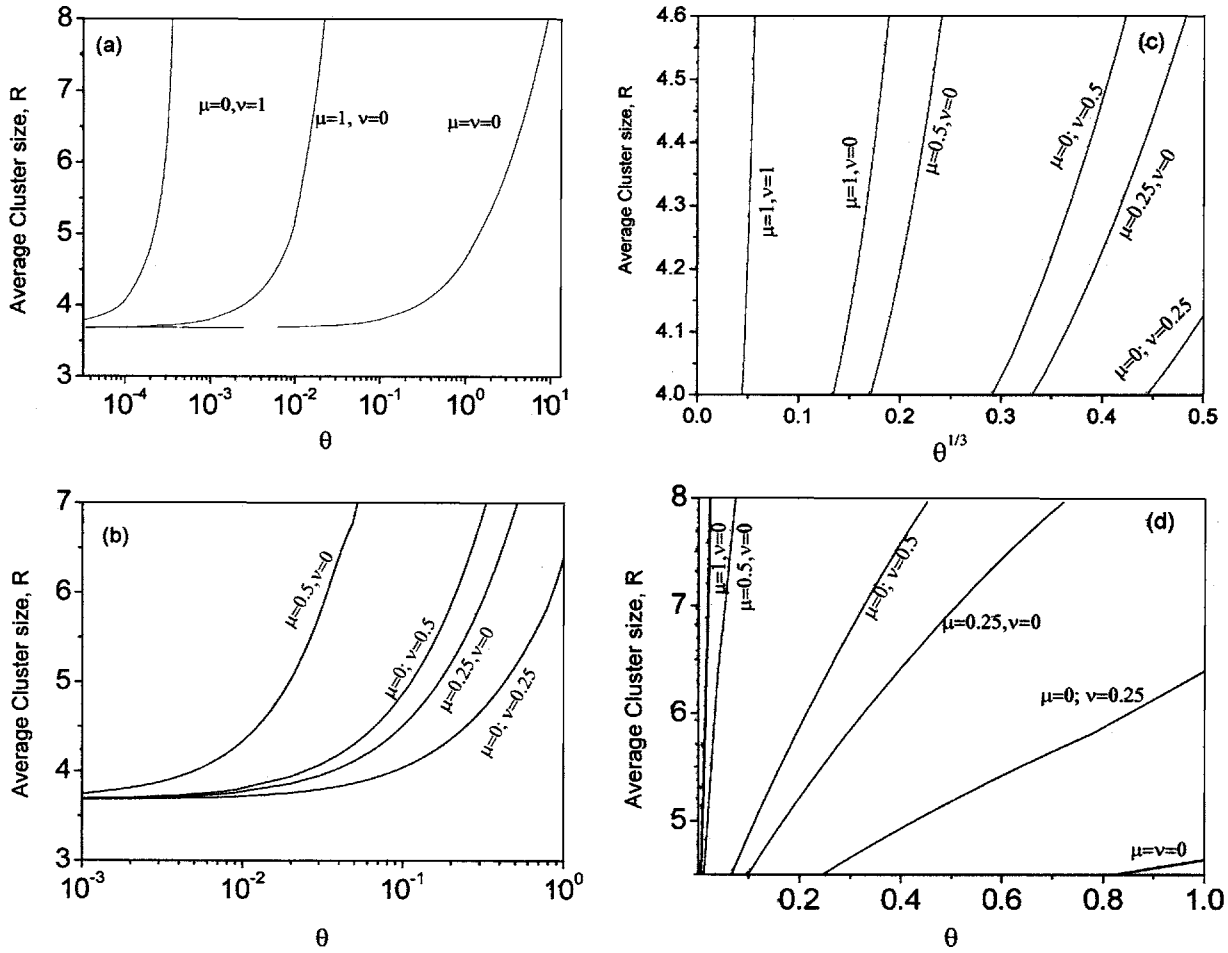

FIG. 3. Time variation of the average cluster size R for (a) systems with analytical solutions and (b) systems solved numerically. (c) A plot versus $\theta^{1/3}$ to show a power-law relationship at early times: (d) A linear plot to show the linear variation at long times.

$\mu=\nu=0$ [i.e., $k_a(x,x')=\kappa$], represents mass independence of the rate coefficient. The zeroth moment based on Eq. (22) is $dC^{(0)}/d\theta=-C^{(0)2}$, which can be solved with the initial condition $C^{(0)}(\theta=0)=C_0^{(0)}$ yielding $C^{(0)}=C_0^{(0)}/(1+C_0^{(0)}\theta)$. Thus, for $\mu=\nu=0$, the average mass of condensed-phase domains can be written in analytical form,

$$C^{\text{avg}}=C_0^{\text{avg}}(1+C_0^{(0)}\theta). \tag{23}$$

The case $\mu=0$ and $\nu=1$ [i.e., $k_a(x,x')=\kappa(x+x')$] represents the coagulation kernel[48,49] and is relevant to branched polymerization processes, where the biparticle interaction depends on the masses of both particles. The zeroth moment based on Eq. (22) is $dC^{(0)}/d\theta=-2C^{(1)}C^{(0)}$, which can be solved with the initial condition $C^{(0)}(\theta=0)=C_0^{(0)}$ yielding $C^{(0)}=C_0^{(0)}\exp(-2C_0^{(1)}\theta)$. Thus, for $\mu=0$ and $\nu=1$, the analytical solution is

$$C^{\text{avg}}=C_0^{\text{avg}}\exp(2C_0^{(1)}\theta). \tag{24}$$

The case $\nu=0$ with μ not equal to zero represents the kernel[50] where the biparticle interaction has a power-law dependence on the size of interacting particles. For instance, $\nu=0$ with $\mu=1$ represents the kernel commonly encountered when polymers react to form crosslinks and has been shown to lead to the phase transition known as gelation.[51] The substitution of $\mu=1$ and $\nu=0$ into Eq. (22) yields for the zeroth moment $dC^{(0)}/d\theta=-C^{(1)2}$, which can be solved with the initial condition $C^{(0)}(\theta=0)=C_0^{(0)}$ yielding $C^{(0)}=C_0^{(0)}-C_0^{(1)2}\theta$. Thus for $\mu=1$ and $\nu=0$ the corresponding analytical solution for C^{avg} is

$$C^{\text{avg}}=C_0^{\text{avg}}/(1-C_0^{\text{avg}}C_0^{(1)}\theta). \tag{25}$$

For other values of μ and ν, analytical solutions are not possible. If the cluster size distribution follows a certain distribution function, a closure approximation[51] can be used to solve the equations. However, a general approach is to solve the equations numerically based on methods described earlier.[45] The differential equation (20) was solved by Runge-Kutta technique with an adaptive time step with $C(\xi,\theta)$ evaluated at each time step sequentially. The mass variable (ξ) was divided into 5000 intervals and the adaptive time (θ) step varied from 10^{-5} to 10^{-2}. These values ensured stability and accuracy at all values of the parameters. At every time step, the mass balance [Eq. (15)] was verified. The numerical results were further validated by comparison with analytical moment solutions.

III. RESULTS AND DISCUSSION

We investigate a range of μ and ν values to explore the kinetics of phase transition in spinodal decomposition. The initial conditions of the first two moments are assumed to be

$C_0^{(0)}=1$ and $C_0^{(1)}=50$. Figures 2(a) and 2(b) show the effects of μ and ν, respectively, on the time evolution of average mass of the condensed phase. The solid lines are numerical solutions, which match well with the available analytical moment solutions (represented by symbols). The average mass increases sharply as μ increases, while the effect is less pronounced with increasing ν. However, in all cases, the condensed-phase domains coalesce and finally evolve into one single phase, which is consistent with the pattern evolution of phase separation via spinodal decomposition.[34] As in experimental observations, the increase of average mass is slow at small times but becomes rapid at larger times.

Since the initial critical size of the condensed-phase domain, ξ^*, is less than 1, c_0^{avg} is the mass of a single molecule, x_m. For spherical dense phase domains, the average characteristic length is

$$R(\theta) = (3/4\ C^{\text{avg}}/N\pi\rho)^{1/3} = \alpha(C^{\text{avg}}(\theta))^{1/3}, \tag{26}$$

where ρ stands for the density of the dense phase domains and N is Avogadro's number. For simulation, α is assumed to be of the order unity. Figure 3(a) shows the time evolution of the average size of the dense phase domains, R, for the three cases having analytical solutions [based on Eqs. (23)–(25)]. The time variation of R is also plotted for various values of μ and ν [Fig. 3(b)] for the numerical solutions. The plot indicates that the time variation of the average size of the condensed-phase domain has a power-law relationship, with the exponent increasing gradually from 1/3 at short times to unity at longer times. To further illustrate this, Fig. 3(a) and 3(b) are replotted against $\theta^{1/3}$ [Fig. 3(c)] at short times and against θ [Fig. 3(d)] at longer times. The plots are nearly linear, indicating that the model successfully predicts the two time regions observed experimentally.[33] Thus this model, which includes aggregation but ignores fragmentation, is able to simulate the time evolution of the average size of the dense phase domains showing both the diffusion-controlled and convection-controlled regimes.

IV. CONCLUSION

Understanding the mechanism of spinodal decomposition is crucial in developing a valid model for the phase-transition kinetics within the spinodal curve. Unlike condensation from a metastable state, we hypothesize that when the classical energy barrier for nucleation is negligible, single molecules aggregate and phase separate rapidly. In the present work, the detailed quantitative description of the phase separation is obtained by cluster-size-distribution kinetics. Focusing on the aggregation mechanism, we have established and solved a generalized population balance equation. For specific integer values of the mass exponents, μ and ν, analytical solutions are obtained. The population balance equation with varying values of μ and ν was solved numerically. The solutions were successful in demonstrating that the average size of the dense phase domains increases as a power law with an exponent of 1/3 at shorter times and linearly at longer times.

[1] N. Goldenfeld, *Lectures on Phase Transitions and the Renormalization Group* (Perseus, Reading, MA, 1992), p. 221.
[2] J. W. Cahn, Acta Metall. **9**, 795 (1961).
[3] J. W. Cahn, Acta Metall. **10**. 179 (1962).
[4] F. J. Alexander, S. Chen, and D. W. Grunau, Phys. Rev. B **48**. 634 (1993).
[5] D. J. Seol, S. Y. Hu, Y. L. Li, J. Shen, K. H. Oh, and L. Q. Chen, Acta Mater. **51**, 5173 (2003).
[6] V. Ruth and J. P. Hirth, J. Chem. Phys. **88**, 7079 (1988).
[7] J. Mainville, Y. S. Yang, K. R. Elder, and M. Sutton, Phys. Rev. Lett. **78**, 2787 (1997).
[8] P. G. de Gennes, J. Chem. Phys. **72**, 4756 (1980).
[9] X. Wang and N. Mashita, Polymer **45**, 2711(2004).
[10] R. Becker and W. Doring, Ann. Phys. **24**, 919 (1935).
[11] I. M. Lifshitz and J. Slyozhov, J. Phys. Chem. Solids **19**, 35 (1961).
[12] C. Wagner, Z. Elektrochem. **65**, 243 (1961).
[13] O. Penrose and J. L. Lebowitz, in *Fluctuation Phenomena*, Studies in Statistical Mechanics Vol. VII, edited by E. W. Montroll and J. L. Lebowitz (North-Holland, Amsterdam, 1976).
[14] J. A. Marqusee and J. Ross, J. Chem. Phys. **79**, 373 (1983).
[15] P. Laurençot and S. Mischler, J. Stat. Phys. **106**, 957 (2002).
[16] C. D. Bolton and J. A. D. Wattis, J. Phys. A **35**. 3183 (2002).
[17] M. von Smoluchowski, Phys. Z. **17**. 557 (1916).
[18] L. Monette and W. Klein, Phys. Rev. Lett. **68**, 2336 (1992).
[19] G. Madras and B. J. McCoy, J. Chem. Phys. **117**, 8042 (2002).
[20] G. Madras and B. J. McCoy, Chem. Eng. Sci. **58**, 2903 (2003).
[21] J. W. Cahn and J. E. Hilliard, J. Chem. Phys. **28**, 258 (1958).
[22] J. W. Cahn and J. E. Hilliard, J. Chem. Phys. **31**, 688 (1959).
[23] K. Binder, H. L. Frisch, and J. Jackle, J. Chem. Phys. **85**, 1505 (1986).
[24] F. F. Abraham and J. A. Barker, J. Chem. Phys. **63**, 2266 (1975).
[25] F. F. Abraham, J. Chem. Phys. **64**, 2660 (1978).
[26] K. T. Moore, W. C. Johnson, J. M. Howe, H. I. Aaronson, and D. R. Veblen, Acta Mater. **50**, 943 (2002).
[27] W. Hu, D. Frenkel, and V. B. Mathot, J. Chem. Phys. **118**, 10343 (2003).
[28] L. Cheng, Phys. Rev. B **58**, 5266 (1998).
[29] W. Hu and D. Frenkel, Macromolecules **37**, 4336 (2004).
[30] R. A. L. Jones, L. J. Norton, E. J. Kramer, F. S. Bates, and P. Wiltzius, Phys. Rev. Lett. **66**, 1326 (1991).
[31] G. Krausch, C. A. Dai, E J Kramer, and F. S. Bates, Phys. Rev. Lett. **71**, 3669 (1993).
[32] P. Wiltzius and A. Cumming, Phys. Rev. Lett. **66**, 3000 (1991).
[33] O. T. Valls and J. E. Farrell, Phys. Rev. E **47**, R37 (1993).
[34] F. Califano and R. Mauri, Ind. Eng. Chem. Res. **43**, 349 (2004).
[35] S. Puri, J. Phys.: Condens. Matter **17**, R101 (2005).
[36] S. Puri and H. L. Frisch, J. Phys.: Condens. Matter **9**, 2109 (1997).
[37] K. Binder, J. Non-Equilib. Thermodyn. **23**, 1 (1998).
[38] P. Guenoun, D. Beysens, and M Robert, Phys. Rev. Lett. **65**, 2406 (1990).
[39] A. J. Bray, Adv. Phys. **43**, 357 (1994).
[40] M. Geoghegan and G. Krausch, Prog. Polym. Sci. **28**, 261 (2003).
[41] D. W. Oxtoby, J. Phys.: Condens. Matter **4**, 7627 (1992).
[42] R. B. McClurg and R. C. Flagan, J. Colloid Interface Sci. **228**, 194 (1998).
[43] G. Madras and B. J. McCoy, Chem. Eng. Sci. **59**, 2753 (2004).
[44] R. Gupta, R. Mauri, and R. Shinnar, Ind. Eng. Chem. Res. **38**, 2418 (1999).
[45] J. Yang, B. J. McCoy, and G. Madras, J. Chem. Phys. **122**, 064901 (2005).
[46] J. Yang, B. J. McCoy, and G. Madras, J. Chem. Phys. **122**, 244905 (2005).
[47] J. Yang, B. J. McCoy, and G. Madras, J. Phys. Chem. **109**, 18550 (2005).
[48] R. D. Vigil and R. M. Ziff, J. Colloid Interface Sci. **133**, 257 (1989).
[49] R. M. Ziff and E. D. McGrady, J. Chem. Phys. **82**, 5296 (1985).
[50] G. Madras and B. J. McCoy, J. Colloid Interface Sci. **246**, 356 (2002).
[51] R. Li and B. J. McCoy, Macromolecules **38**, 6742 (2005).